

Journal of Mathematical Extension  
Vol. 17, No. 2, (2023) (3)1-25  
URL: <https://doi.org/10.30495/JME.2023.2503>  
ISSN: 1735-8299  
Original Research Paper

## Kaiser Window Efficiency in Calculating the Exact Fractal Dimension by the Power Spectrum Method

**M. R. Shamsyeh Zahedi\***

Payame Noor University

**S. Mohammadi**

Payame Noor University

**A. Heydari**

Payame Noor University

**Abstract.** In this article, exact fractals is investigated using the power spectrum method and wavelets. In the proposed algorithms, we use Daubechies and Symlet wavelets of orders 3 to 8 and show the efficiency of the Kaiser window function in the more accurate calculation of the exact fractal dimension. The comparison of the results obtained by the box-counting method on two types of accurate fractals investigated recently shows that the power spectrum and wavelet method using the Kaiser window filter has higher accuracy.

**AMS Subject Classification:** MSC code 1; MSC code 2; more

**Keywords:** Power Spectrum, Fractal Dimension, Wavelet Transform, Kaiser Window

---

Received: September 2022; Accepted: February 2023

\*Corresponding Author

## 1 Introduction

There are forms in nature that, while complex, follow a certain order. Mandelbrot first called these shapes fractal and called the geometry of these shapes fractal geometry. Fractal word is derived from the Latin word fractus, whose root is from the words fraction and fragment, which means irregular or fragmented. In explaining his theory by choosing the term fractal, Mandelbrot has, in fact, emphasized one of the main characteristics of these geometric shapes, which arises from the nature of their fragmentation. According to him, the universe and all natural phenomena are a kind of fractal. The clouds are not spherical; the mountains are not like cones; the sea shores are not circular; the bark of the tree is not smooth; and the lightning does not move in a straight line [20].

Clark and Schweizer pointed out that fractal geometry is one of the four most important scientific concepts of the twentieth century, which is equivalent to quantum mechanics, the theory of general relativity, and the two-helix model in the structure of DNA [9].

Fractal models have been used in a variety of image processing and pattern recognition applications. For example, several researchers have used fractal techniques to describe image textures and different segment types of images [8, 15, 21, 24].

Models of fractal were applied to study the scaling behavior of geographic features, and the knowledge generated by this type of research can be used to determine the optimal resolution of pixels and polygons used in remote sensing and GIS applications [3, 6, 15, 24].

The fractal Lipschitz condition is given on the  $F^\alpha$ -calculus, which applies for the nondifferentiable function in the sense of the standard calculus. Picard iterative process in the  $F^\alpha$ -calculus has an important role in the numerical and approximate solution of fractal differential equations. The fractal Picard iteration method is introduced for finding the local solution of a fractal differential equation [10].

The Fourier transforms used in the field of frequency analysis, the Laplace transforms generalizing the Fourier transform to the complex domain, and the Sumudu transforms preserving Taylor coefficients, are examples of integral transforms, which have applications in applied mathematics, physics, and engineering. Sumudu transforms preserve units

and the scaling property of domains and transform linear differential equations to algebraic ones [11].

Fractals are geometrical objects such that their fractal dimension exceeds their topological dimension. Fractals as models can be found in many applications in science and engineering. Analogous nonlocal fractional derivatives on the real line and fractal nonlocal derivatives were defined on fractal sets for modeling processes with memory effects such as the elastic modulus of the fractal structure materials. The variance of random walks on fractals, which has an important role in anomalous diffusion processes, shows the fractional power law relationship [12].

Local fractional derivatives are needed in many physical problems. The effort of defining local fractional calculus leads to a new measure of fractals. In view of this new measure, the  $C^\mu$ -Calculus was formulated for totally disconnected fractal sets and nondifferentiable fractal curves. The stability and asymptotic behavior of fractal differential equations have an important role in various applications in science and engineering [29].

Fractional calculus has an important role in modeling various fascinating complex phenomena in the form of ordinary or partial differential equations. Many researchers worked on developing the fractional calculus concept and investigating new ways to define fractional derivatives, which range from Riemann–Liouville to new hybrid proportional–Caputo fractional derivatives. They used an elementary fractional differential equation to discover that their new operator is deeply connected with the bivariate Mittag–Leffler function, which arises naturally from the modeling of certain systems of the real world [2].

Many physical systems can store information on the state component's derivative, and these systems are referred to as neutral systems. Many real-world systems and biological procedures exhibit some form of dynamic actions, with continuous and discrete properties. these systems (such as market crashes, earthquakes, and epidemics) can experience some jump-type stochastic perturbations. Such systems have the nonexistence of continuous sample paths. Consequently, stochastic processes with jumps are well-matched to modeling such models [1].

The most essential tool for examining the epidemiological features of viral diseases is the mathematical model. Regarding the dynamics of the

illness, it may offer some insightful information. Several scholars have undertaken various investigations using various studies concerning the modeling and the dynamical study of the rotavirus disease's transmission [22].

Partial differential equations are among the best mathematical tools for analyzing spatiotemporal processes. These nonlinear equations deal with nonlinearity and dispersive effects at the same time and are one of the simplest forms of evolution equations. These nonlinear equations are widely used for the description of dynamics of localized stationary along with pulsating waves envelopes. These nonlinear equations are known as universal equations because they explain how waves move through many physical systems. These equations are crucial tools for comprehending the physical analogies and variations in the nonlinear behavior of dispersive waves [25].

The fractional heat equation is one of the most well-known fractional partial differential equations that describe the physical phenomenon. In recent years, solving the fractional heat equation magnetized the attention of mathematicians because of its importance [23].

There are two categories of fractals (self-similar and self-affine). In self-similar fractals, the component shape bears a striking resemblance to the overall shape. This component grows in a constant proportion in all directions and forms the whole. Nevertheless, in a self-affine fractal, the component shape does not grow at a constant rate in all directions [19, 20].

To understand fractal geometry, we must find a way to show the complexity of the shape in numbers. This number is the same as the fractal dimension [5].

According to fractal application and fractal phenomena, different methods have been proposed to calculate the fractal dimension, including the box-counting method [4], the Higuchi method [13], the Fourier power spectrum method [19, 20], and the generalized box-counting method [17].

Wu et al. [32] proposed a method based on fractal production (box-counting) and box determination with a mathematical definition to eliminate box scale deviation. The known fractals (Koch curve and Sierpinski triangle) were analyzed to confirm this method, which is close to the

actual value of the fractal dimension.

So et al. [27] presented a box-counting algorithm in combination with a new sampling method and a fractional box-counting method. To solve the margin problem that occurs for images with any size, the fraction box-counting method allows the number of frames to be real instead of integers. This method is applied to known fractal images (Koch curve and Sierpinski triangle) with an exact fractal dimension that is close to their true value.

In the power spectrum method, the algorithm used to analyze self-affine fractals is more accurate than the following methods:

- 1) Fractal Picard Iteration [10],
- 2) Sumudu Transforms [11],
- 3) Fractal nonlocal derivatives [12],
- 4) Fractal differential equations [29],
- 5) Caputo fractional derivatives [2],
- 6) Stochastic Processes such as market crashes, earthquakes, and epidemics [1],
- 7) Fractional heat equation [23].

Exact fractals are a type of self-similar fractals with a special form of self-affine fractals. Recently, algorithms have been developed to calculate the dimension of such fractals by the box-counting method. Let exact fractals be only artificial phenomena in mathematics, and we mostly deal with fractals in nature. In this article, using wavelets and the power spectrum method, we will calculate the dimension of such fractals by presenting an algorithm. Then, to check the effectiveness of this algorithm, we calculate the exact dimension of fractals. As we know, the exact dimension of these fractals can be theoretically calculated in mathematics. In this algorithm, Daubechies and Symlet wavelets with orders of 3 to 8 have been used.

To improve the answer and calculate the fractal dimension more accurately by this algorithm, we use the window function called the Kaiser window. The structure of the article is set as follows. In Section 2, the power spectrum and wavelet methods are introduced to obtain the fractal dimension. In Section 3, we introduce two types of exact fractals (Koch curve and Sierpinski triangle). The introduction of the Kaiser window for its use in the fractal dimension calculation algorithm

is mentioned in Section 4. In Section 5, we compare the numerical results obtained by the power spectrum and wavelet method with the box-counting method. In the end, in Section 6, conclusions and suggestions for future work are presented.

## 2 Power and Wavelet Spectrum Methods

In this section, the power spectrum and wavelet method are introduced. The powers of each Fourier component are called the power spectral density (power spectrum). They are usually calculated by using a technique called the fast Fourier transform [14, 28]. For self-affine signals (self-affine signals are a rescaled version of a small part of the signal that has the same statistical distribution as the larger part), the power spectrum density  $S(f)$  is proportional to the frequency  $f$ , as shown in equation (1). In the following equation, the value of the power spectrum coefficient ( $\alpha$ ) can be obtained as a linear regression slope applied to the power spectrum in the logarithmic coordinate system [14, 20, 26, 30]:

$$S(f) \sim f^{-\alpha} \rightarrow \alpha = \frac{-\log S(f)}{\log f}. \quad (1)$$

After calculating the power spectral coefficient from equation (1), to obtain the fractal dimension [19, 26], one can use the following equation:

$$D = \frac{5 - \alpha}{2} = 2 - H, \quad (2)$$

where  $H$  is called the Hurst parameter, which defines the fractal structure.

In the power spectrum method, wavelets can be used to replace the analyzed data in Fourier analysis. Wavelets are a group of mathematical functions that are used to decompose a signal into its frequency components, the resolution of each component being equal to its scale. Wavelet transform is the decomposition of a function based on wavelet functions. Compared to the Fourier transform, it can be said that the wavelet has a very good localization characteristic. That is, the wavelet not only determines the amount of frequencies in the signal but also determines when those frequencies occur in the signal [33].

### 3 Introduction of Two Exact Fractals and Their Dimensions Calculations

In this section, we first introduce the box-counting method for calculating the fractal dimension and then introduce the exact fractals.

In the box-counting method, the covering effect of a curve (the feature of filling the space with a curve) is investigated with a set of area elements. In this way, with the given sizes of the elements of the area of a box, how many boxes are needed to cover the curve completely? Finally, when the size of the elements of the area tends to zero, the total area of the area covered by the area of the boxes will converge to the size of the curve. Therefore, the following equation is used to calculate the fractal dimension:

$$D = \lim_{r \rightarrow 0} \frac{\log N}{\log \frac{1}{r}}. \quad (3)$$

In equation (3),  $r$  represents the number of boxes, and  $N(r)$  equals the number of boxes used to divide the curve into specific sizes [4].

Now we introduce the two exact fractals and analyze their dimensions.

#### 3.1 Koch curve

The Koch curve is generated with the help of a line segment and applying an algorithm, as can be seen in Figure 1. We consider a line segment of length one. The generator ( $k = 1$ ) is made of 4 parts, and each part is  $1/3$  the length of the initiator, whose length is 1. The second-order ( $k = 2$ ) Koch curve replaces each of the four generating segments with the same shape, so it has 16 small segments, and each segment is  $1/9$  unit in length. That is, the total length of the quadratic curve is  $4/3$ .

We can calculate dimension  $D$  by looking at how the number of units,  $N$ , changes with the magnification factor  $r$ . In this case, we see that the number of parts in the generator  $N$  is 4 and that the magnification factor is 3 because each part of the generator is  $1/3$  unit in length. The same relationship exists between each of the curve orders (different  $k$ ).

Therefore, according to relation (3), we can say [18, 20]  $D = \log(4)/\log(1/3) = 1.26$ .

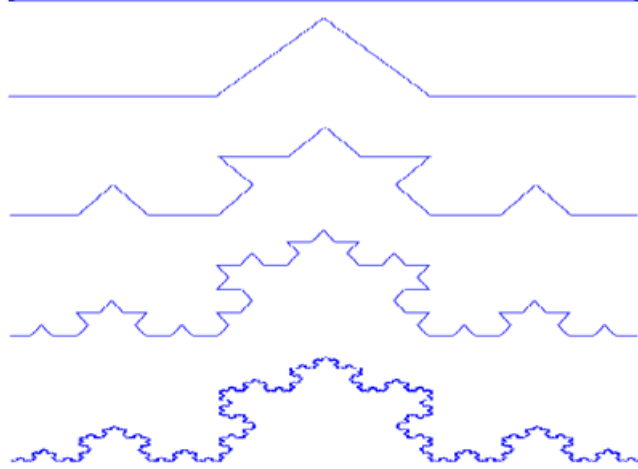


**Figure 1:** Koch curve

### 3.2 Sierpinski triangle

In the Sierpinski triangle (Figure 2), the shape consists of three similar components. If we represent the original shape with  $A$  and the small components with  $a$ , we have

$$A = 3 \times a. \quad (4)$$

On the other hand, the length of each small component is half of the original shape. So the magnification scale in this figure is  $1/2$ . We have

$$a = A\left(\frac{1}{2}\right)^d, \quad (5)$$

where  $d$  is the dimension. By substituting (5) in (4), we have [18]

$$\begin{aligned} A &= 3 \times A\left(\frac{1}{2}\right)^d, \\ 1 &= 3 \times \frac{1}{2^d}, \\ 2^d &= 3 \rightarrow d = \frac{\log 3}{\log 2} = 1.5850. \end{aligned} \quad (6)$$

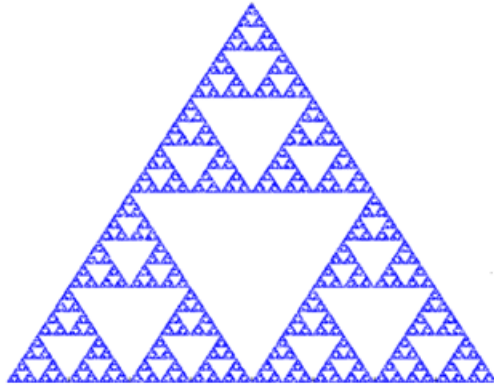


**Figure 2:** Sierpinski Triangle

## 4 Kaiser Window

In this section, we introduce the Kaiser window.

The window function is a mathematical function having zero values outside the selected interval. When another function is multiplied by a window function, the out-of-range product also becomes zero. All that remains is the overlapping section. "view through the window," the use of window function, power spectrum analysis, and filter design can be mentioned [16, 31, 33].

The series used in the signal processing is symmetrical about the axis ( $t = 0$ ). The Fourier transform of an even or symmetric signal is even, so the frequency content of the windows is symmetric about the axis ( $w = 0$ ). The main peak of the Fourier transform of the windows is located at the frequency ( $w = 0$ ), which decays to zero with oscillations. To increase the frequency of resolution, the power value of the series should be concentrated near ( $w = 0$ ) [33].

A suitable window in the frequency domain has a narrow main peak and no sub-peaks (frequency leakage), and it drops off quickly at high frequencies. If a good frequency of resolution is required, then a rectangular window should be chosen. However, this enhancement of frequency resolution causes frequency leakage, which requires windows with sub-peak areas that descend at a high rate to reduce the leakage [33].

The Kaiser window is optimal in terms of having the highest power value in the main lobe for a given sidelobe amplitude [16].

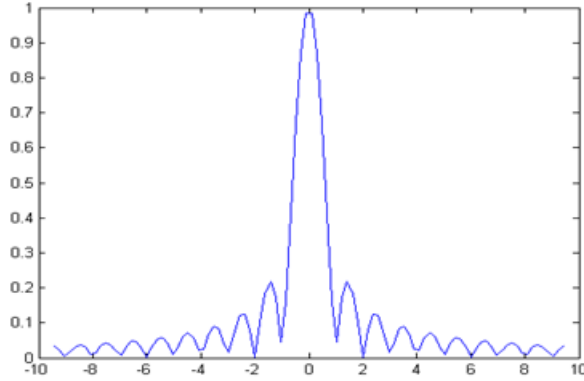


**Figure 3:** Kaiser Function

The general form of the Kaiser Window function is as follows:

$$w(\beta, n) = \begin{cases} \frac{I_0\{\beta[1-(\frac{2n}{N-1})^2]^{\frac{1}{2}}\}}{I_0(\beta)}, & -\frac{N-1}{2} \leq n \leq \frac{N-1}{2}, \\ 0, & \text{otherwise.} \end{cases} \quad (7)$$

In equation (7),  $N$  is the window length, and  $I_0(x)$  is the modified Bessel function for the first type of zero arrangement, defined as follows:

$$I_0(x) = \sum_{k=0}^x \left[ \frac{x(k)}{2} \right]^2 \frac{1}{k!}.$$

Also, the beta parameter ( $\beta$ ) determines the shape of the window, which controls the balance between the width of the main lobe and the amplitude of the side lobes [16].

## 5 Numerical Results and Conclusions

In this section, we want to discuss the results obtained from the exact fractal dimension using the power spectrum method and compare the

results with the box-counting method.

In [32], the presented method is based on the analysis of points generated by mathematical expression and defining the length of the sides of the boxes instead of pixels. It helps a lot to break the pixel limitation and brings the result closer to the theoretical results.

In [27], the method is based on the combination of a new sampling method and a fractional box-counting method. To solve the problem of wasted pixels, the fractional box-counting method allows the number of boxes to be real rather than an integer. The results related to the estimation of the fractal dimension of the Koch curve and the Sierpinski triangle by the box-counting method in [27, 32] and comparing it with the theoretical value are given in Table 1.

**Table 1:** Comparison of the estimation of the fractal dimension of the Koch curve and the Sierpinski triangle

$D_{exact}$ =The value of the fractal dimension of the Koch curve and the Sierpinski triangle based on the theoretical method, respectively, 1.261859 and 1.584962				
	Theoretical fractal dimension value	Numeric fractal dimension value	Error rate	Reference
Sierpinski Triangle	$D_{exact} = 1.584962$	$D_{numerical} = 1.584995$	0.0021%	[32]
	$D_{exact} = 1.585$	$D_{numerical} = 1.266430$	0.126%	[27]
Koch Curve	$D_{exact} = 1.261859$	$D_{numerical} = 1.266430$	0.3622%	[32]
	$D_{exact} = 1.262$	$D_{numerical} = 1.267$	0.3962%	[27]

Now, using the power spectrum method mentioned in Section 2, we calculate the dimension of two exact fractals. In this method, by using the wavelet transformation applied in exact fractals, we obtain the power graph in terms of frequency. Then we calculate the slope of its logarithmic graph line, using equation (2) for the fractal dimension of the curve. Since, in the power spectrum method, the main part of the algorithm in calculating the fractal dimension is the calculation of the

power of the given series (the series of generating points of the fractal curve), we use the optimality property of the Kaiser window function in calculating the power of a series. In this regard, we can reduce the error rate and bring the answer closer to the true value of the exact fractal dimension.

**Table 2:** Fractals Type

Slope= $\alpha$	Fractal type	Value of $H$
$\alpha < -3$	Bias	–
$-3 < \alpha < -1$	Differentiated fractional Gaussian noise	$H = \frac{(\alpha + 3)}{2}$
$-1 < \alpha < +1$	Fractional Gaussian noise	$H = \frac{(\alpha + 1)}{2}$
$\alpha = 0$	Brownian motion	$H = 0.5$
$1 < \alpha < 3$	Fractional Brownian motion	$H = \frac{(\alpha - 1)}{2}$
$3 < \alpha < 5$	Integrated fractional Brownian motion	$H = \frac{(\alpha - 3)}{2}$
$\alpha > 5$	Bias	–

The data in Table 2 are used to determine the type of fractal and the value of the Hurst parameter of the Koch curve and the Sierpinski triangle [7].

In presenting the numerical results, the length of the Kaiser window of Daubechies and Symlet wavelets of orders 3 to 8 in the Koch curve for  $k$  (the number of self-similar steps) equal to 3 to 12 was analyzed and investigated. In this analysis, it can be seen that with the increase of  $k$ , the length of the Kaiser window ( $m$ ) increases. The reason for increasing the length of the Kaiser window is the use of the applied wavelets with different orders. In the power spectrum method, it can be seen that we approach the real value of the fractal dimension of the Koch curve with high accuracy in the following cases:

1. Third-order Daubechies for  $k$  equal to 6, 11, and 12.
2. Fourth-order Daubechies for  $k$  equal to 6, 7, 10, and 12.

3. Fifth-order Daubechies for  $k$  equal to 7, 11, and 12.
4. Seventh-order Daubechies for  $k$  equal to 8.
5. Eighth-order Daubechies for  $k$  equal to 7 and 8.
6. Third-order Symlet for  $k$  equal to 6, 11, and 12.
7. Fifth-order Symlet for  $k$  equal to 7, 11, and 12.
8. Sixth- and Eighth-orders Symlet for  $k$  equal to 6, 7, and 11.

By using the power spectrum method according to the wavelet used in the calculation algorithm, the data and output of the results related to the Koch curve are given in Tables 3–10 and Figure 4.

**Table 3:** Third-order Daubechies and Symlet

The number of self-similar steps $k$	Kaiser window $m$	Numeric fractal dimension value $D$	Error $E$
6	700	1.2619	0.00325%
7	1900	1.2621	0.01918%
8	6373	1.2620	0.01117%
9	25023	1.2618	0.00467%
10	110020	1.2616	0.02052%
11	465030	1.2618	0.00467%
12	1800030	1.2618	0.00467%

**Table 4:** Fourth-order Daubechies

The number of self-similar steps $k$	Kaiser window $m$	Numeric fractal dimension value $D$	Error $E$
6	506	1.2619	0.00325%
7	1703	1.2619	0.00325%
8	5968	1.2616	0.02052%
9	25033	1.2620	0.01117%
10	110010	1.2618	0.00467%
11	460045	1.2617	0.0126%
12	1800150	1.2618	0.00467%

**Table 5:** Fifth-order Daubechies

The number of self-similar steps $k$	Kaiser window $m$	Numeric fractal dimension value $D$	Error $E$
7	1766	1.2619	0.00325%
8	6151	1.2615	0.02845%
9	25848	1.2617	0.0126%
10	114655	1.2617	0.0126%
11	479360	1.2618	0.00467%
12	1788999	1.2618	0.00467%

**Table 6:** Seventh-order Daubechies

The number of self-similar steps $k$	Kaiser window $m$	Numeric fractal dimension value $D$	Error $E$
7	1739	1.2622	0.02702%
8	6086	1.2618	0.00467%
9	25541	1.2620	0.01117%
10	113310	1.2620	0.01117%
11	474090	1.2617	0.0126%
12	1774250	1.2621	0.01909%

**Table 7:** Eighth-order Daubechies

The number of self-similar steps $k$	Kaiser window $m$	Numeric fractal dimension value $D$	Error $E$
7	1741	1.2619	0.003254%
8	6131	1.2618	0.00467%
9	25985	1.2620	0.01117%
10	110020	1.2616	0.02052%
11	460030	1.2618	0.00467%
12	1800250	1.2617	0.0126%

**Table 8:** Fifth-order Symlet

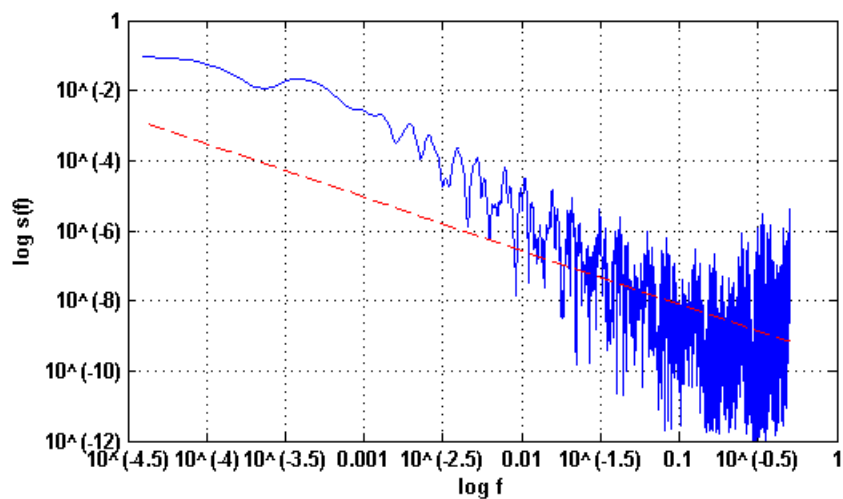
The number of self-similar steps $k$	Kaiser window $m$	Numeric fractal dimension value $D$	Error $E$
6	678	1.2620	0.00325%
7	1781	1.2619	0.00325%
8	6360	1.2617	0.0126%
9	27090	1.2617	0.0126%
10	125511	1.2617	0.0126%
11	542030	1.2618	0.00467%
12	1938250	1.2618	0.00467%

**Table 9:** Sixth-order Symlet

The number of self-similar steps $k$	Kaiser window $m$	Numeric fractal dimension value $D$	Error $E$
6	777	1.2619	0.00325%
7	1742	1.2619	0.00325%
8	6226	1.2615	0.02845%
9	25025	1.2617	0.0126%
10	110030	1.2616	0.02052%
11	460030	1.2618	0.00467%
12	1877300	1.2616	0.02052%

**Table 10:** Eighth-order Symlet

The number of self-similar steps $k$	Kaiser window $m$	Numeric fractal dimension value $D$	Error $E$
6	738	1.2619	0.00325%
7	1868	1.2619	0.00325%
8	6190	1.2620	0.01117%
9	25005	1.2622	0.02702%
10	110030	1.2617	0.0126%
11	460030	1.2618	0.00467%
12	1800350	1.2616	0.02052%

**Figure 4:** Logarithmic diagram of the fractal dimension of the Koch curve

By applying the power spectrum method and using the type of wavelet used in the algorithm, the data and results related to the Sierpinski triangle are written in Tables 11–12 and Figures 5–6.

**Table 11:** Data of the Sierpinski triangle for Daubechies Wavelet

$D_{exact} = 1.584962$					
Wavelet	Power spectrum coefficient $\alpha$	Hurst $H$	Numeric fractal dimension value $D$	Kaiser window $m$	Error $E$
Third-order Daubechies	-0.16734	0.4163	1.5837	44600	0.08%
Fourth-order Daubechies	-0.17001	0.4150	1.5850	43599	0.0024%
Fifth-order Daubechies	-0.17023	0.4149	1.5851	45014	0.0087%
Sixth-order Daubechies	-0.16858	0.4157	1.5843	42599	0.04%
Seventh-order Daubechies	-0.16219	0.4189	1.5811	35903	0.2%
Eighth-order Daubechies	-0.17362	0.4132	1.5868	49000	0.1%

**Table 12:** Data of the Sierpinski triangle for Symlet Wavelet

$D_{exact} = 1.584962$					
Wavelet	Power spectrum coefficient $\alpha$	Hurst $H$	Numeric fractal dimension value $D$	Kaiser window $m$	Error $E$
Third-order Symlet	-0.16998	0.4150	1.5850	44597	0.0024%
Fourth-order Symlet	-0.17001	0.4150	1.5850	43599	0.0024%
Fifth-order Symlet	-0.1693	0.4154	1.5846	43000	0.02%
Sixth-order Symlet	-0.17045	0.4148	1.5852	49603	0.01%
Seventh-order Symlet	-0.17286	0.4136	1.5864	47604	0.09%
Eighth-order Symlet	-0.16993	0.4150	1.5850	48000	0.0024%

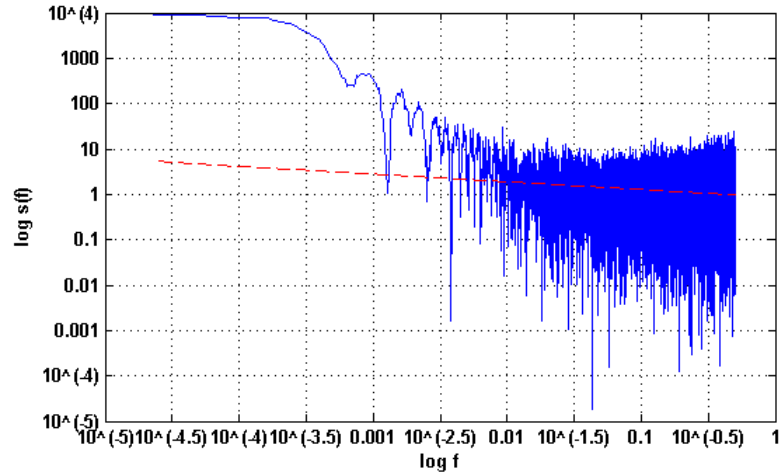


**Figure 5:** Fourth-order Daubechies in the analysis of the fractal dimension of the Sierpinski triangle

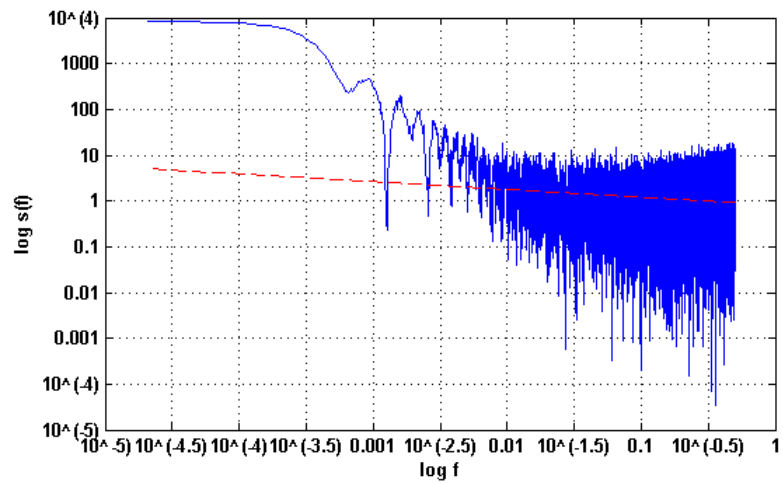


**Figure 6:** Eighth-order Symlet in the analysis of the fractal dimension of the Sierpinski triangle

The range of dimension changes in the power spectrum method us-

ing wavelets in the Koch curve is (1.2622, 1.2615), while the value of the fractal dimension of the Koch curve in [32] and [27] is 1.266430 and 1.2670, respectively. Regarding Sierpinski's triangle, the range of changes is (1.5858, 1.5811), and the values obtained in [32] and [27] are 1.5854995 and 1.5830, respectively. According to Tables 11 and 12, it can be seen the real value of the fractal dimension of the Sierpinski triangle with higher accuracy than the results obtained in [27, 32], in the fourth-order Daubechies wavelet, third-order Symlet, fourth-order Symlet, and eighth-order Symlet approaches.

## 6 Conclusion

In this article, exact fractals were analyzed by applying the power spectrum method and using wavelets. In this method and the proposed algorithm, we used the Kaiser window filter. It was observed that the results obtained after applying the Kaiser window are closer to the real value of the exact fractal dimension. To better understand the accuracy of this method, we compared the results with the box-counting method, which was recently reviewed in [27, 32] on two types of accurate fractals. These results showed that using the power spectrum and wavelet method with the help of the Kaiser window has higher accuracy. In future work, we suggest using the power spectrum method and the proposed algorithm in this article to investigate the fractal dimension of the solution of chaotic systems.

## References

- [1] Q. T. Ain, M. Nadeem, A. Akgül, and M. De la Sen, Controllability of impulsive neutral fractional stochastic systems, *Symmetry*, 14.12 (2022), 2612.
- [2] N. Attia, A. Akgül, D. Seba, A. Nour, M.D. la Sen, and M. Bayram, An efficient approach for solving differential equations in the frame of a new fractional derivative operator, *Symmetry*, 15.1 (2023), 144.

- [3] M. F. Barnsley, Iterated function systems, *In Chaos and Fractals: Mathematics Behind the Computer* (1989), 127–144 (Providence, RI: American Mathematical Society).
- [4] J. Brewer and L. D. Girolamo, Limitations of fractal dimension estimation algorithms with implications for cloud studies, *Atmospheric Research*, 82 (2006), 433–454.
- [5] F. M. Brojeni and A. Maleki, The role of fractal geometry in the study and analysis of time series waveforms, *the third national conference of new ideas in electrical engineering*, (2014) (In Persian).
- [6] K. C. Clarke and D. M. Schweizer, measuring the fractal dimension of natural surfaces using a robust fractal estimator, *Cartography and Geographic Information Systems*, 18 (1991), 37–47.
- [7] A. Dauphiné, *Fractal Geography*, John Wiley & Sons, (2013).
- [8] S. M. De Jong and P. A. Burrough, A fractal approach to the classification of Mediterranean vegetation types in remotely sensed images, *Photogrammetric Engineering and Remote Sensing*, 61 (1995), 1041–1053.
- [9] U. Freiberg and S. Kohl, Box dimension of fractal attractors and their numerical computation, *Communications in Nonlinear Science and Numerical Simulation*, 95 (2021): 105615.
- [10] A. K. Golmankhaneh and C. Tunç, On the Lipschitz condition in the fractal calculus, *Chaos, Solitons and Fractals*, 95 (2017), 140–147.
- [11] A. K. Golmankhaneh and C. Tunç, Sumudu transform in fractal calculus, *Applied Mathematics and Computation*, 350 (2019), 386–401.
- [12] A. K. Golmankhaneh and C. Tunç, Stochastic differential equations on fractal sets, *Stochastics*, 92.8 (2020), 1244–1260.
- [13] T. Higuchi, Approach to an irregular time series on the basis of the fractal theory, *Physica D*, 31 (1998), 277–283.

- [14] H. Karkovska and A. Karkovska, *Fractal dimension of self-affine signals: four methods of estimation*, arXiv preprint arXiv:1611.06190 (2016).
- [15] J. M. Keller, S. Chen and R. M. Crownover, Texture description and segmentation through fractal geometry, *Computer Vision, Graphics, and Image Processing*, 45 (1989), 150–166.
- [16] A. A. Kumar *Digital Signal Processing*, PHI Learning Pvt. Ltd., (2014).
- [17] G. Li, K. Zhang, J. Gong and X. Jim, Calculation method for fractal characteristics of matching topography surface based on wavelet transform, *Procedia CIRP* 79 (2019): 500–504.
- [18] S. Lynch, *Dynamical Systems with Application Using MATLAB*, second edition, Springer, (2014).
- [19] B. D. Malamud and D. L. Turcotte, Self-affine time series: Measures of weak and strong persistence, *Journal of Statistical Planning and Inference*, 80 (1999), 173–196.
- [20] B. B. Mandelbrot, *the Fractal Geometry of Nature*, Vol. 1. New York: WH freeman, (1982).
- [21] S. W. Myint, Fractal approaches in texture analysis and classification of remotely sensed data: Comparisons with spatial autocorrelation techniques and simple descriptive statistics, *International Journal of Remote Sensing*, 24 (2003), 1925–1947.
- [22] S. Naowarat, S. Ahmad, S. Saifullah, M.D.L. Sen, and A. Akgül, Crossover dynamics of Rotavirus disease under fractional piecewise derivative with vaccination effects: Simulations with real data from Thailand, West Africa, and the US, *Symmetry*, 14.12 (2022), 2641.
- [23] M. Partohaghighi, A. Akgül, E.K. Akgül, N. Attia, M. De la Sen, and M. Bayram, Analysis of the fractional differential equations using two different methods, *Symmetry*, 15.1 (2023), 65.

- [24] A. P. Pentland, Fractal-based descriptions of natural scenes, *IEEE Transactions on Pattern Analysis and Machine Intelligence*, 6 (1984), 661–674.
- [25] A. Sarwar, M. Arshad, M. Farman, A. Akgül, I. Ahmed, M. Bayram, S. Rezapour, and M. De la Sen, Construction of novel bright-dark solitons and breather waves of unstable nonlinear Schrödinger equations with applications, *Symmetry*, 15.1 (2023), 99.
- [26] M. Shamsyeh Zahedi and J. Zail, Fractal dimension and navigational information provided by natural scenes, *PLoS One*, 13.5 (2018): e0196227.
- [27] G. B. So, H. R. So, and G. G. Jin, Enhancement of the box-counting algorithm for fractal dimension estimation, *Pattern Recognition Letters*, 98 (2017), 53–58.
- [28] W. Sun, G. Xu, P. Gong and S. Liang, Fractal analysis of remotely sensed images: A review of methods and applications, *International Journal of Remote Sensing*, 27 (2006), 4963–4990.
- [29] C. Tunç, A. K. Golmankhaneh, and Urmia Branch, On stability of a class of second alpha-order fractal differential equations, *AIMS math*, 5.3 (2020), 2126–2142.
- [30] R. F. Voss, Random fractal forgeries, *Earnshaw R. A. (Ed.), Berlin: Springer*, (1985), 805–835.
- [31] E. W. Weinstein, *CRC Concise Encyclopedia of Mathematics*, CRC Press, (2003).
- [32] J. Wu, X. Jin, S. Mi, and J. Tang, An effective method to compute the box-counting dimension based on the mathematical definition and intervals, *Results in Engineering*, 6 (2020): 100106.
- [33] D. Yonesian and M. Valikhani, *Wavelet transform and its applications in railway engineering*, University of Science and Technology publications, (2014) (In Persian).

**Moosarreza Shamsyeh Zahedi**

Associate Professor of Mathematics

Department of Mathematics

Payame Noor University (PNU), P.O.Box 19395-4697, Tehran, Iran.

E-mail: m.s.zahedi@pnu.ac.ir

**Siavash Mohammadi**

Ph.D. student of Mathematics

Department of Mathematics

Payame Noor University (PNU), P.O.Box 19395-4697, Tehran, Iran.

E-mail: phd.mohammadi.s@pnum.ac.ir

**Aghileh Heydari**

Professor of Mathematics

Department of Mathematics

Payame Noor University (PNU), P.O.Box 19395-4697, Tehran, Iran.

E-mail: A.heidari@pnu.ac.ir